REPORT DOCUMENTATION PAGE	*Form Approved* *OMB No. 0704-0188*

1. REPORT DATE *(DD-MM-YYYY)* 6/21/2018	**2. REPORT TYPE** Final Technical	**3. DATES COVERED** *(From - To)* 7/01/2014 - 6/30/2018

4. TITLE AND SUBTITLE
Early Student Support for a Process Study of Oceanic

Responses to Typhoons

5a. CONTRACT NUMBER

5b. GRANT NUMBER
N00014-14-1-0360

5c. PROGRAM ELEMENT NUMBER

6. AUTHOR(S)
Ren-Chieh Lien

5d. PROJECT NUMBER

5e. TASK NUMBER

5f. WORK UNIT NUMBER

7. PERFORMING ORGANIZATION NAME(S) AND ADDRESS(ES)
University of Washington – Applied Physics Laboratory
4333 Brooklyn Avenue NE
Seattle, WA 98105-6613

8. PERFORMING ORGANIZATION REPORT NUMBER

9. SPONSORING / MONITORING AGENCY NAME(S) AND ADDRESS(ES)
Office of Naval Research (Code 32)
875 North Randolph Street
Arlington, VA 22203-1995

10. SPONSOR/MONITOR'S ACRONYM(S)
ONR

11. SPONSOR/MONITOR'S REPORT NUMBER(S)

12. DISTRIBUTION / AVAILABILITY STATEMENT:

Distribution Statement A: Approved for public release; distribution is unlimited.

13. SUPPLEMENTARY NOTES
This project is funded to support a PhD student. He obtained his PhD degree in December 2017 and has been working as a postdoc in CSIRO, Australia since February 2018.

14. ABSTRACT

Drag coefficients beneath Typhoon Megi in the western Pacific are computed using velocity measurements made by EM-APEX floats, and measurements of the 10-m wind. Downwind drag coefficients increase to $3.7 \pm 0.2 \times 10^{-3}$ at 31 m/s, a value greater than most previous estimates, but decrease to $1.8 \pm 0.1 \times 10^{-3}$ for wind speeds > 45 m/s, in agreement with previous estimates. At wind speeds 30-45 m/s, significant crosswind wind stress is found such that the wind stress vector is about 20 degree clockwise from the 10-m wind vector. This method is applied to five sets of EM-APEX float measurements taken under 5 different tropical cyclones. In all cases, the surface wind stress vector rotates clockwise from the 10-m wind vector. The largest downwind drag coefficient occurs in the front-right sector of the moving storms. The variation of drag coefficient is explained by the variation of wave breaking under different wave forcing regimes. Surface wave peak frequency and significant wave height under Typhoon Fanapi are computed using float measurements assuming JONSWAP spectrum. Float estimates of peak frequency are 10-20% less than WAVEWATCH III (ww3) model results, and differences of significant wave height between float estimates and ww3 results are mostly < 2 m.

15. SUBJECT TERMS
Wind Stress, Drag Coefficient, Extreme Wind Speed, Surface Wave, Tropical Cyclone, EM-APEX Float, Cross-Wind Stress

16. SECURITY CLASSIFICATION OF:			**17. LIMITATION OF ABSTRACT**	**18. NUMBER OF PAGES**	**19a. NAME OF RESPONSIBLE PERSON**
					Ren-Chieh Lien
a. REPORT Unclassified	**b. ABSTRACT** Unclassified	**c. THIS PAGE** Unclassified	UU	9	**19b. TELEPHONE NUMBER** *(include area code)* (206) 543-1300

Early Student Support for a Process Study of Oceanic Responses to Typhoons

Ren-Chieh Lien
Applied Physics Laboratory
University of Washington
1013 NE 40th Street
Seattle, Washington 98105
Phone: (206) 685-1079 fax: (206) 543-6785 email: lien@apl.washington.edu

Award Number: N00014-14-1-0360

LONG-TERM GOALS

Our long-term scientific goals are to understand the upper ocean dynamics, to understand the coupling between the ocean and atmosphere via air–sea fluxes, and to quantify the mechanisms of air–sea interactions. Our ultimate goal is to help develop improved parameterizations of air–sea fluxes in ocean–atmosphere models and parameterizations of small-scale processes in the upper ocean and the stratified interior.

OBJECTIVES

Tropical cyclones derive energy from the ocean via air–sea fluxes. Oceanic heat content in the mixed layer and the air–sea enthalpy flux play important roles in determining the storm's maximum potential intensity, structure, energy, trajectory, and dynamic evolution. The most energetic oceanic responses to tropical cyclone forcing are surface waves, wind-driven currents, shear and turbulence, and inertial currents. Quantifying the effect of these oceanic processes on air–sea fluxes during tropical cyclone passage will aid understanding of storm dynamics and structure. The ocean's recovery after tropical cyclone passage depends upon small- and meso-scale oceanic processes in the storm's wake region. These processes are the least understood primarily because of the paucity of direct field observations under passing tropical cyclones; consequently, there are large uncertainties in air–sea flux parameterizations in extreme wind regimes.

This project supports a graduate student, Andy Hsu, to pursue a Ph.D. in Physical Oceanography. He earned a M.S. degree in spring 2014 and obtained a Ph.D. degree in December 2017. The major scientific goals of his Ph.D. study are to (1) quantify the surface wind stress and drag coefficients under extreme winds, (2) quantify surface waves under extreme winds, and (3) parameterize effects of surface waves on drag coefficients under moving tropical cyclones.

Surface wind stress is often computed using a drag coefficient (C_d). The parameterization of C_d is critical for studies of air–sea interaction. For example, the maximum potential intensity (MPI) of tropical cyclones is inversely proportional to C_d. Previous studies derive empirical formulas for C_d as a function of wind speed at 10 m above the sea surface ($\mathbf{U}_{10}$). Recent studies suggest that C_d may also depend on surface gravity wave properties, which vary greatly in different sectors of tropical cyclones. It remains a challenge to parameterize effects of surface waves on C_d

accurately. This study proposes a new parameterization, which includes the effects of surface waves and wind speed on drag coefficients under moving storms.

ACCOMPLISHMENTS

The graduate student, Andy Hsu, successfully completed a Ph.D. program in December 2017. After graduation, he continued to work on data analysis and preparing publications. Presently, he is working at CSIRO as a postdoctoral researcher. Two papers were published. One summarized results of drag coefficients measured under Typhoon Megi (2010), and the other described an improved broad-band spectral method for estimating surface wave properties under typhoons. A third paper is in preparation; it summarizes drag coefficients under five tropical cyclones and proposes a new parameterization including the effects of surface waves and surface wind speed on drag coefficients under moving tropical cyclones. Significant results of these three papers are briefly summarized as follows.

Surface Wind Stress and Drag Coefficients in Typhoon Megi

Estimates of drag coefficients beneath Typhoon Megi (2010) are calculated from roughly hourly velocity profiles of three EM-APEX floats, air-launched ahead of the storm, and from air-deployed dropsondes and microwave measurements of the 10-m wind field (Fig. 1). The profiles are corrected to minimize contributions from tides and low-frequency motions and thus isolate the current induced by Typhoon Megi. Surface wind stress is computed from the linear momentum budget in the upper 150 m. Three-dimensional numerical simulations of the oceanic response to Typhoon Megi indicate that with small corrections, the linear momentum budget is accurate to 15% before the passage of the eye, but cannot be applied reliably thereafter. Monte Carlo error estimates indicate that stress estimates can be made for wind speeds greater than 25 m s^{-1}; the error decreases with greater wind speeds. Downwind and crosswind drag coefficients are computed from the computed stress and the mapped wind data (Fig. 2). Downwind drag coefficients increase to $3.5\pm0.7 \times 10^{-3}$ at 31 m s^{-1}, a value greater than most previous estimates, but decrease to $2.0\pm0.4 \times 10^{-3}$ for wind speeds > 45 m s^{-1}, in agreement with previous estimates. The crosswind drag coefficient of $1.6\pm0.5 \times 10^{-3}$ at wind speeds 30–45 m s^{-1} implies that the wind stress is about 20° clockwise from the 10-m wind vector and thus not directly downwind as is often assumed.

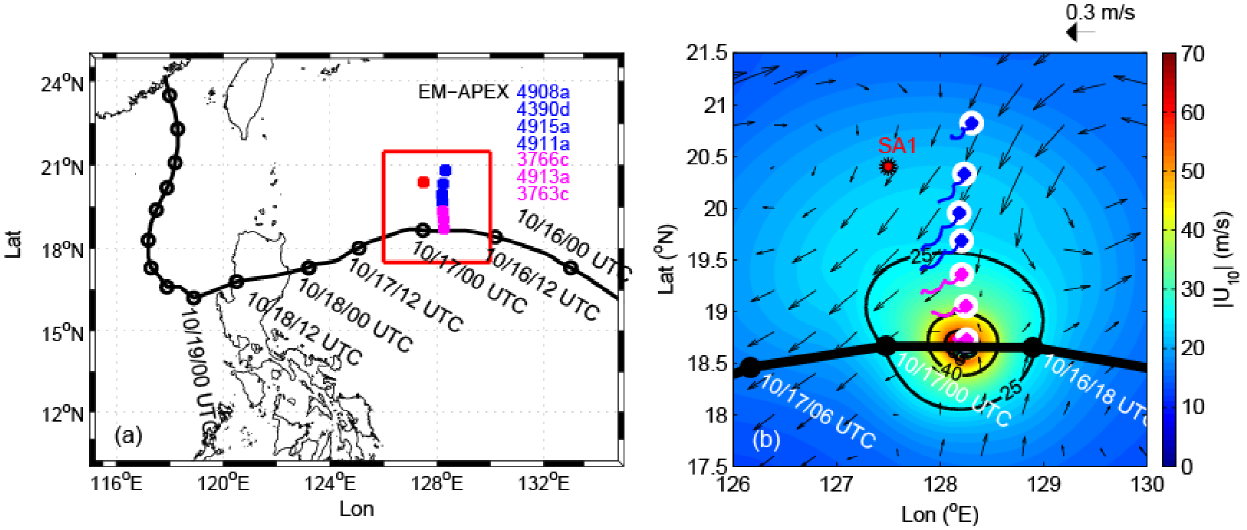

Figure 1: (a) Typhoon Megi's track (black curve with dots), deployment positions of EM-APEX floats (blue and magenta dots), and position of a mooring SA1 (red dot), and (b) the wind map of wind speed at 10 m above the sea surface (color shading) at 20:30 UTC 16 October at the arrival time of Typhoon Megi at the float array, AVISO surface geostrophic current velocity (black arrows) on 17 October, EM-APEX float positions and trajectories (blue and magenta dots and curves), and mooring SA1 position (red dot). Typhoon track is labeled with time as month/day/hour UTC. Floats at locations marked as magenta dots are used to compute drag coefficients.

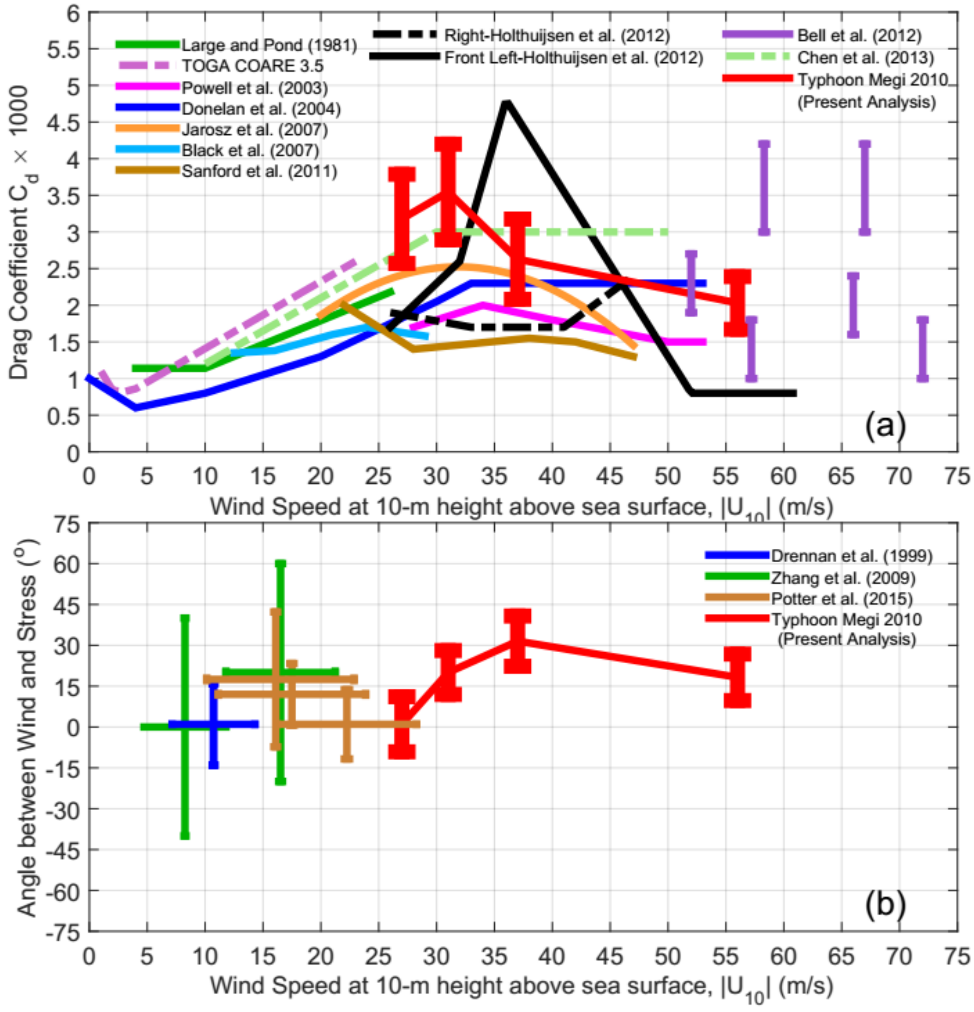

Figure 2: The drag coefficient C_d as a function of wind speed at 10 m above the sea surface $\left|\overrightarrow{U_{10}}\right|$ from Hsu et al. (2017) and as proposed by previous investigators (other colors). (b) Angle between the surface wind and stress vectors from our analysis (heavy red) and from Drennan et al. (1999, Fig. 6), Zhang et al. (2009, Figs. 1 and 3) and Potter et al. (2015, Figs. 1 and 4). Measured wind speed from these investigators is extrapolated to 10 m above the sea surface assuming a logarithmic wind profile. The horizontal and vertical bars describe the ranges of their data. The positive angle implies a stress vector that points clockwise from the wind vector.

Estimates of Surface Waves From Subsurface EM-APEX Floats Under a Typhoon

Seven subsurface EM-APEX floats measured the voltage induced by the motional induction of sea water under Typhoon Fanapi (2010). Voltage measurements were processed to estimate high-frequency oceanic velocity variance $\widetilde{\sigma_u}^2(z)$ associated with surface gravity waves. Surface wave peak frequency f_p and significant wave height H_s are estimated by nonlinearly least-squared fitting to $\widetilde{\sigma_u}^2$, assuming a broadband JONSWAP surface wave spectrum. The H_s is further corrected for the effects of the floats' rotation, earth geomagnetic field's inclination, and surface wave propagation direction. The f_p is 0.08–0.10 Hz, with the maximum at the rear-left quadrant ~

0.02 Hz higher than that at the rear-right quadrant of Fanapi. The H_s is 6– 2 m, with the maximum at the rear sector of Fanapi. Comparing our estimates of f_p and H_s with those estimated assuming a single dominant surface wave in a previous study, the differences of f_p and H_s between the two methods can be more than 0.02 Hz and 4 m, respectively. The surface waves under Fanapi are simulated in the WAVEWATCH III (ww3) model to assess and compare with float estimates (Fig. 3). The difference of surface wave spectrum between JONSWAP and ww3 leads to the uncertainties of < 5% outside Fanapi's eyewall, and > 10% within the eyewall. The estimates of f_p are 10% less than simulated f_p^{ww3} before the passage of Fanapi's eye, and 20% less after eye passage. Most differences between H_s and simulated H_s^{ww3} are < 2 m, except those at the rear-left quadrant of Fanapi, ~ 5 m. We conclude that improving ww3 surface wave simulations is important to future studies of tropical cyclone–wave–ocean interactions.

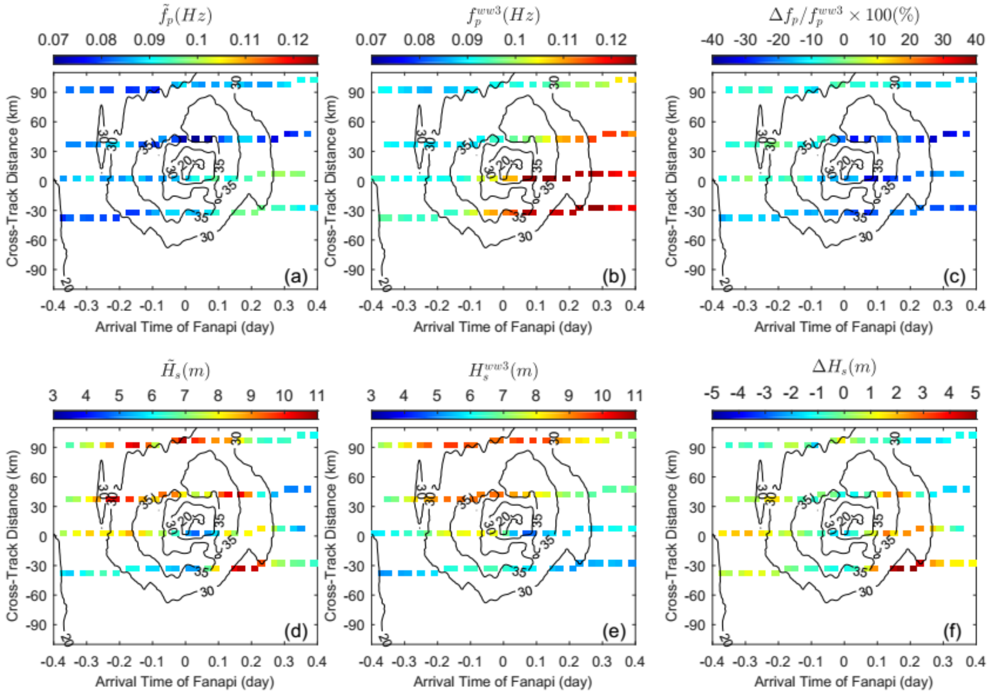

Figure 3: Maps of EM-APEX floats' estimated peak frequency $\widetilde{f_p}$ (a) and significant wave height $\widetilde{H_s}$ (d), and the ww3 model outputs of f_p^{ww3} (b) and H_s^{ww3} (e). The ratio $\Delta f_p/f_p^{ww3}$ ($\Delta f_p = \widetilde{f_p} - f_p^{ww3}$) and ΔH_s ($\Delta H_s = \widetilde{H_s} - H_s^{ww3}$) are shown in (c) and (f), respectively. Black contour lines show the wind speed at 10-m above the sea surface. The abscissa shows the relative arrival time of Typhoon Fanapi' eye to the float array. The ordinate is the distance of floats' positions to Fanapi's track.

Scaling of Drag Coefficients Under Five Tropical Cyclones

Surface wind stress $\boldsymbol{\tau}$ estimated using ocean current measurements taken by thirteen EM-APEX floats beneath the forward half of five tropical cyclones (Fig. 4) and aircraft measurements of winds $\mathbf{U_{10}}$ are used to compute the downwind drag coefficient $\widetilde{C_{\parallel}}$ and the angle ϕ from the $\mathbf{U_{10}}$ to the $\boldsymbol{\tau}$ (> 0 clockwise orientated). We report significant scattering of $\widetilde{C_{\parallel}}$ between storms, and the large $\phi > 30°$ (Fig. 5). A non-dimensional effective wind duration, a function of $|\mathbf{U}_{10}|$, storm translation speed, and float positions to eyes, predicts $\widetilde{C}_{\parallel}$ to 25%. These dependences are explained by variations in wave breaking under differing wave forcing regimes. The proposed parameterization of drag coefficients will be useful for guiding the future atmosphere–wave–-ocean coupling models used to predict the intensification of tropical cyclones.

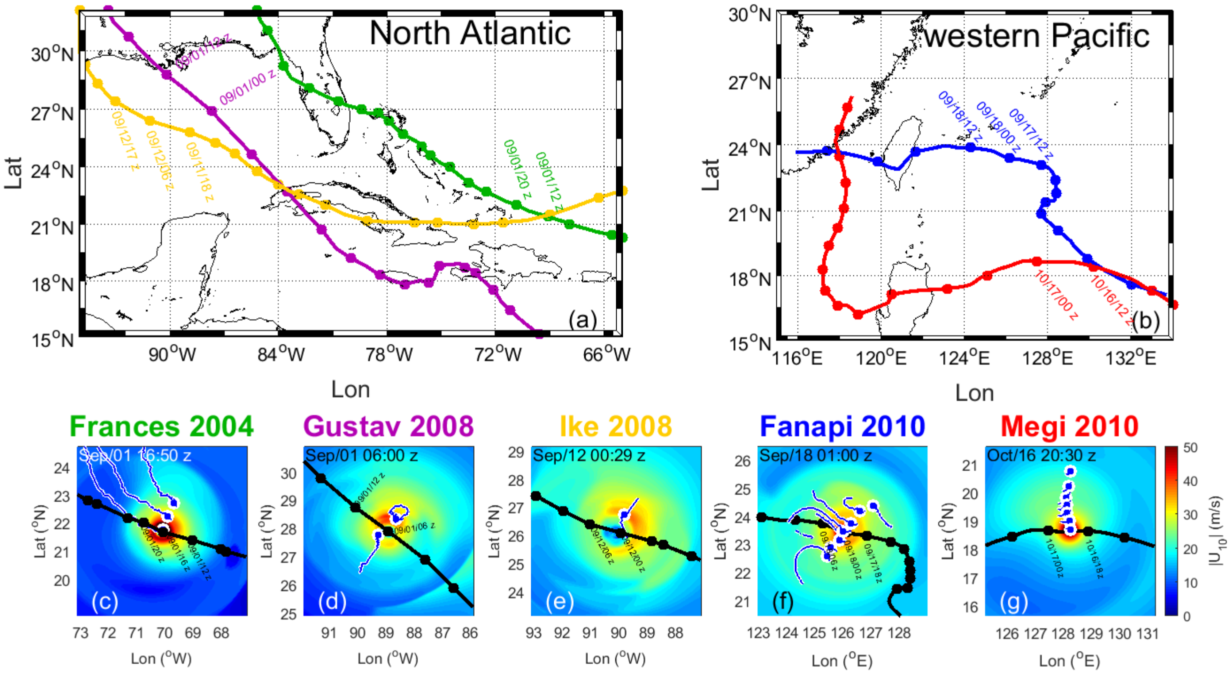

Figure 4: The tracks of hurricanes in the North Atlantic (a), Frances: green; Gustav: purple; Ike: gold. The tracks of typhoons in the western Pacific (b), Fanapi: blue; Megi: red. Tropical cyclone wind maps at the time eyes pass near EM-APEX float positions (c–g) and trajectories of float positions (blue dots connected with lines in c–g). The colored dots connected with thick lines in (a) and (b) are tracks of tropical cyclone eyes every 12 h, and the black dots connected with a thick line in (c)–(g) are tracks of tropical cyclone eyes every 6 h.

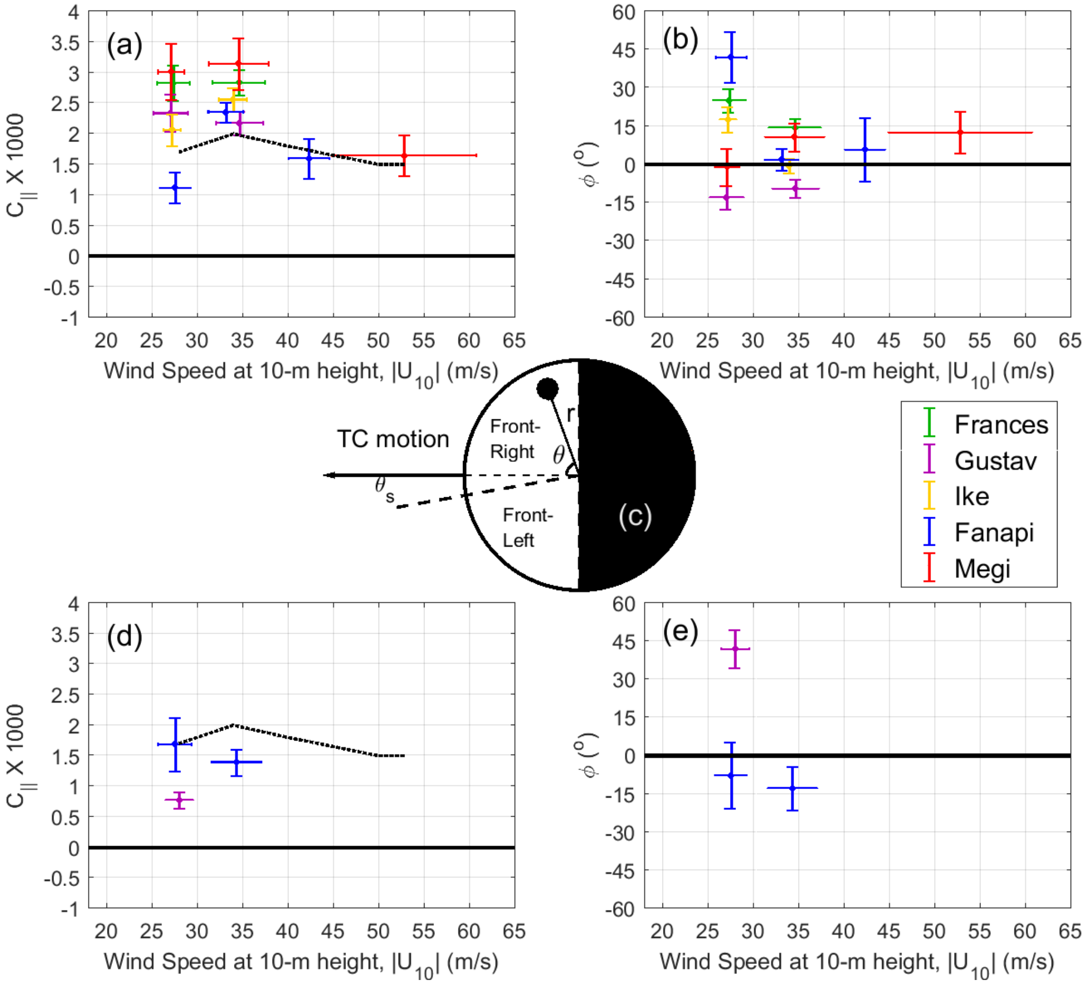

Figure 5: Estimates of adjusted downwind drag coefficient $\widetilde{C}_{\parallel}$ (a and d) and the angle ϕ (b and e) between the surface wind stress $\tilde{\boldsymbol{\tau}}$ and wind $\mathbf{U}_{10}$ in five different tropical cyclones, using the float measurements in the front-right (a and b) and front-left (d and e) sectors of tropical cyclones (c). The vertical error bars represent the standard deviations of $\widetilde{C}_{\parallel}$ averages and ϕ, respectively, and the horizontal error bars represent the standard deviations of interpolated $|\mathbf{U}_{10}|$ at the float positions. The boundary between two sectors is defined assuming $\theta_s = -10°$. For the positions of the floats, the azimuth $\theta > 0$ is clockwise from tropical cyclones' motion, and r the distance of floats to the tropical cyclone's eye. Black dashed lines are results using the Powell et al. (2003) drag coefficient.

IMPACT/APPLICATION

Tropical cyclones cause strong oceanic responses, e.g., surface waves, inertial waves, and a deepening of the surface mixed layer. To improve the modeling skill of oceanic responses to tropical cyclones and the prediction of tropical cyclones, we need to understand the small-scale processes responsible for the air–sea fluxes and interior oceanic mixing, and the meso-scale oceanic processes that modulate the background oceanic heat content. The ITOP field experiment provides direct observations of oceanic responses forced by tropical cyclones and the ocean's recovery, as well as aids understanding of the dynamics of small- and meso-scale oceanic processes. These observations will help improve the prediction skill of oceanic and atmospheric models in high wind regimes.

REFERENCES

Bell, M. M., M. T. Montgomery and K. A. Emanuel (2012). Air–sea enthalpy and momentum exchange at major hurricane wind speeds observed during CBLAST. *J. Atmos. Sci*., **69**(11), 3197-3222.

Black, P. G., E. A. D'Asaro, T. B. Sanford, W. M. Drennan, J. A. Zhang, J. R. French, P. P. Niiler, E. J. Terrill and E. J. Walsh (2007). Air–sea exchange in hurricanes: synthesis of observations from the coupled boundary layer air–sea transfer experiment. *Bull. Amer. Meteorol. Soc*., **88**(3): 357-374.

Chen, S. S., W. Zhao, M. A. Donelan and H. L. Tolman (2013). Directional wind–wave coupling in fully coupled atmosphere–wave–ocean models: Results from CBLAST-Hurricane. *J. Atmos Sci*., **70**(10): 3198-3215.

Donelan, M. A., B. K. Haus, N. Reul, W. J. Plant, M. Stiassnie, H. C. Graber, O. B. Brown and E. S. Saltzman (2004). On the limiting aerodynamic roughness of the ocean in very strong winds. *Geophys. Res. Lett*., **31**(18), doi: 10.1029/2004GL019460

Drennan, W. M., H. C. Graber and M. A. Donelan (1999). Evidence for the effects of swell and unsteady winds on marine wind stress. *J. Phys. Oceanogr*., **29**(8): 1853-1864.

Edson, J. B., V. Jampana, R. A. Weller, S. P. Bigorre, A. J. Plueddemann, C. W. Fairall, S. D. Miller, L. Mahrt, D. Vickers and H. Hersbach (2013). On the exchange of momentum over the open ocean. *J. Phys. Oceanogr*., **43**(8): 1589-1610.

Holthuijsen, L. H., M. D. Powell, and J. D. Dietrazak (2012). Wind and waves in extreme hurricanes. *J. Geophys. Res.- Oceans*, **117**, C09003, doi:10.1029/2012JC007983.

Jarosz, E., D. A. Mitchell, D. W. Wang and W. J. Teague (2007). Bottom-up determination of air-sea momentum exchange under a major tropical cyclone. *Science*, **315**(5819): 1707-1709.

Large, W.G., and S. Pond (1981). Open ocean momentum flux measurements in moderate to strong winds. *J. Phys. Oceanogr*., **11**, 324-336.

Powell, M. D., P. J. Vickery, and T. A. Reinhold (2003). Reduced drag coefficient for high wind speeds in tropical cyclones. *Nature*, **422**, 279–283.

Price, J. F., T. B. Sanford and G. Z. Forristall (1994). Forced stage response to a moving hurricane. *J. Phys. Oceanogr*., **24**, 233-260.

Sanford, T. B., J. F. Price, and J. B. Girton (2011). Upper-ocean response to Hurricane Frances (2004) observed by profiling EM-APEX Floats. *J. Phys. Oceanogr*., **41**, 1041–1056, doi: 10.1175/2010JPO4313.1.

Zhang, F. W., W. M. Drennan, B. K. Haus and H. C. Graber (2009). On wind-wave-current interactions during the Shoaling Waves Experiment. *J. Geophy. Res.-Oceans*, **114**(C1): C01018.

PUBLICATIONS

Hsu, J.-Y., R.-C. Lien, E. A. D’Asaro, T. B. Sanford (2018). Scaling of drag coefficients under five tropical cyclones. *Geophys. Res. Lett*., to be submitted.

Hsu, J.-Y., R.-C. Lien, E. A. D’Asaro, and T. B. Sanford (2018). Estimates of surface waves

using subsurface EM-APEX floats under Typhoon Fanapi 2010. *J. Atmos. Ocean. Technol.*, **35**, 1053-1075, doi: 10.1175/JTECH-D-17-0121.1

Hsu, J.-Y., R.-C. Lien, E. A. D'Asaro, and T. B. Sanford (2017). Estimates of surface wind stress and drag coefficients in Typhoon Megi. *J. Phys. Oceanogr*., **47**, 545-565, doi: 10.1175/JPO-D-16-0069.1